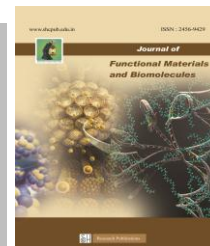




SACRED HEART RESEARCH PUBLICATIONS

# Journal of Functional Materials and Biomolecules

Journal homepage: [www.shcpub.edu.in](http://www.shcpub.edu.in)



ISSN: 2456-9429

## A WIDE BAND GAP $\text{CeO}_2/\text{Nb}_2\text{O}_5$ NANOCOMPOSITE VIA COPRECIPITATION: A PROMISING PHOTOCATALYST MATERIAL

G. Jayakumar<sup>1\*</sup>, P. Sowmiya, A. Dhayal Raj<sup>1</sup>, D. Daniel Lawrence<sup>1</sup>, S. Rahul<sup>1</sup>

Received on 09 October 2025, accepted on 19 November 2025,

Published online on December 2025

### Abstract

Cerium Oxide-Niobium Oxide ( $\text{CeO}_2/\text{Nb}_2\text{O}_5$ ) nanocomposite have been successfully synthesized by coprecipitation method. The properties of the prepared sample are characterized by powder X-ray diffraction analysis, high resolution scanning electron microscopy, Fourier transform infra-red spectroscopy and ultraviolet-visible spectroscopy. From the powder X-ray diffraction, the average crystallite size of  $\text{CeO}_2/\text{Nb}_2\text{O}_5$  nanocomposite is found to be 17 nm. The HRSEM images show that the  $\text{CeO}_2/\text{Nb}_2\text{O}_5$  nanocomposite have spherical morphology and have more agglomeration. From the FTIR spectra, the characteristic peaks confirm that the spectrum with the presence of Cerium oxide and Niobium oxide NPs. The UV-Vis absorption spectra of  $\text{CeO}_2/\text{Nb}_2\text{O}_5$  nanocomposite shows that the absorption peak occurs at 314 nm. From these observations, the prepared wide band gap  $\text{CeO}_2/\text{Nb}_2\text{O}_5$  nanocomposite will be used as a potential photocatalyst.

**Keywords:** Cerium oxide, Niobium oxide, Nanocomposite, spherical shape, agglomeration.

### 1. Introduction

Nanocomposite research represents a pivotal and rapidly advancing frontier within the broader domain of nanoscience, fundamentally concerned with the design, synthesis, and application of multiphase solid materials where at least one constituent phase possesses dimensions in the

nanoscale regime [1-4]. The core principle underpinning this field, as highlighted in foundational texts, is the synergistic combination of at least two distinct materials to create a new substance whose properties are not merely an average of its components but are judiciously modified and often vastly superior, a revolutionary concept that has garnered significant scientific and industrial attention in recent years [5]. This transformative potential arises from the profound physical and chemical phenomena that emerge at the nanoscale, where the drastic increase in surface area-to-volume ratio of the nanomaterials create an immense interfacial area within the composite matrix, be it polymeric, ceramic or metallic, facilitating powerful interactions that fundamentally alter the macroscopic behavior of the final material [6,7]. The successful realization of these advanced materials, however, is critically contingent upon the synthesis methodology, which must overcome the significant challenge of achieving a uniform

\*Corresponding author: E-mail: [gjayaphysics@gmail.com](mailto:gjayaphysics@gmail.com)  
<sup>1</sup>Department of Physics, Sacred Heart College (Autonomous), Tirupattur-635 601, Tamil Nadu, India.

dispersion of the nanoparticles and strong interfacial adhesion to prevent agglomeration, a common pitfall driven by the high surface energy of nanoparticles that can lead to defect points and compromised properties [8]. Among the plethora of synthesis techniques available, including hydrothermal, sol-gel, and laser ablation, the co-precipitation method stands out as a particularly effective and proven wet-chemical route for certain ceramic and metallic nanocomposites, involving the simultaneous precipitation of metal hydroxides from a salt precursor with the help of a base in a solvent, a process characterized by key steps of nucleation, growth, coarsening, and aggregation, where the conditions of high super saturation lead to the formation of a large number of small particles, and where secondary processes like ostwald ripening dramatically affect the final size, morphology, and properties of the product, ultimately yielding a high-purity material with a high yield [9,10]. The transformative impact of nanocomposites is already being felt across a staggering array of industrial sectors, promising to revolutionize the entire business world, as semiconducting nanocomposites are driving innovations in flexible electronics, high-efficiency sensors, and photo detectors. Hence, in the present work is focused on the preparation of cost-effective method of  $\text{CeO}_2 - \text{Nb}_2\text{O}_5$  nanocomposite and the structural and morphological properties are studied and discussed.

## 2. Experimental

### 2.1 Synthesis of $\text{CeO}_2/\text{Nb}_2\text{O}_5$ nanocomposite

The co-precipitation method is employed to synthe-

size  $\text{CeO}_2/\text{Nb}_2\text{O}_5$  nanocomposite. 0.1M of cerium nitrate hexahydrate ( $\text{Ce}(\text{NO}_3)_3 \cdot 6\text{H}_2\text{O}$ ) is dissolved in 100ml of distilled water, and 2 g of Niobium oxide is added to the solution, then stirred using a magnetic stirrer for 30 minutes. 0.2 Mole of Sodium hydroxide ( $\text{NaOH}$ ) is added drop by drop. Finally, the precipitate is washed for 2–3 times with deionized water and ethanol, the resulting precipitate is dried at  $80^\circ\text{C}$  for 12 hours in an oven. Finally, the powder is taken in a silica crucible and annealed in a furnace at  $500^\circ\text{C}$  for 2 hours and a  $\text{CeO}_2/\text{Nb}_2\text{O}_5$  nanocomposite is obtained.

## 3. Results and Discussion

### 3.1 The Powder XRD analysis of $\text{CeO}_2/\text{Nb}_2\text{O}_5$ Nanocomposite

The powder XRD pattern of  $\text{CeO}_2/\text{Nb}_2\text{O}_5$  nanocomposite is depicted in Fig. 1. The powder XRD pattern confirms the formation of  $\text{CeO}_2/\text{Nb}_2\text{O}_5$  nanocomposite. The diffraction peaks at  $28.28^\circ$ ,  $32.28^\circ$ ,  $47.50^\circ$ ,  $58.34^\circ$ , and  $76.80^\circ$  can be indexed to the (111), (200), (220), (311), (311), and (331) planes of the cubic structure  $\text{CeO}_2$  (JCPDS card No. 34-0394). The diffraction peaks at  $24.93^\circ$ ,  $38.09^\circ$ ,  $44.15^\circ$ ,  $54.50^\circ$ ,  $56.20^\circ$ ,  $63.98^\circ$ ,  $66.74^\circ$ ,  $71.92^\circ$  can be indexed to the (440), (211), (721), (831), (602) and (400) plane of hexagonal  $\text{Nb}_2\text{O}_5$  (JCPDS card No.72-1484). This confirms the presence of both cerium and niobium oxide in the prepared composites. The crystallite size of the  $\text{CeO}_2/\text{Nb}_2\text{O}_5$  nanocomposite is calculated by Scherrer formula, the average crystallite size is found to be 17.2 nm.

The calculated crystallite size, dislocation density and

the interplanar spacing of the prepared CeO<sub>2</sub>/Nb<sub>2</sub>O<sub>5</sub> nanocomposite are presented in table 1.

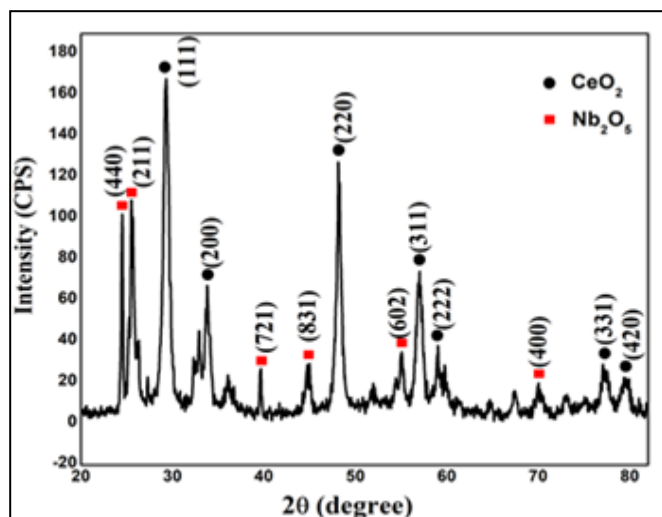


Fig. 1. Powder XRD pattern of CeO<sub>2</sub>/Nb<sub>2</sub>O<sub>5</sub>

Table 3: Calculated crystallite size, dislocation density and d-spacing of prepared CeO<sub>2</sub>/Nb<sub>2</sub>O<sub>5</sub> nanocomposite

2θ (degree)	Reflection (hkl)	FWHM (β)	D (nm)	Dislocation density (δ) (m <sup>-2</sup> )	d spacing distance (Å)
23.86	(101)	0.241	6.1	2.6620	1.5917
24.93	(440)	0.789	9.8	1.0353	1.6619
28.28	(111)	0.893	8.6	1.3472	1.8815
32.28	(431)	0.724	10.5	9.0081	2.1404
32.09	(200)	0.563	13.5	5.4439	2.1282
38.66	(611)	0.680	11.0	8.2467	2.5487
44.15	(831)	0.386	19.1	2.7512	2.8938
47.50	(220)	0.853	8.5	1.3787	3.1011
54.23	(442)	0.786	8.9	1.2365	3.5094
56.20	(311)	0.982	7.1	1.9659	3.6267
58.34	(602)	0.649	10.6	8.7601	3.7531
63.98	(990)	0.503	13.3	5.5773	4.0792
66.74	(312)	0.456	14.5	4.7276	4.2353
71.92	(532)	0.541	11.8	7.0891	4.5406
76.80	(331)	1.107	5.6	3.1639	4.7828

### 3.2 FTIR analysis

The FTIR spectrum of CeO<sub>2</sub>/Nb<sub>2</sub>O<sub>5</sub> nanocomposite was obtained using the KBr pellet method, as publicized in Fig. 2. The weak bands at 1389 cm<sup>-1</sup>, 1564 cm<sup>-1</sup> and 3429 cm<sup>-1</sup> are due to (O-H) stretching vibration of water. The band around 1115 cm<sup>-1</sup> may be due to the (C-O) single

bond stretching mode. The broad band around 1644 cm<sup>-1</sup> is due to the H-O-H bending vibration of water. The spectrum exhibits a strong band at 506 cm<sup>-1</sup>, 844 cm<sup>-1</sup> confirms the (O-Ce-O) stretching vibration of the spectra (ref). The absorption band around 706 cm<sup>-1</sup> is due to the presence of (O-Nb-O) spectra.

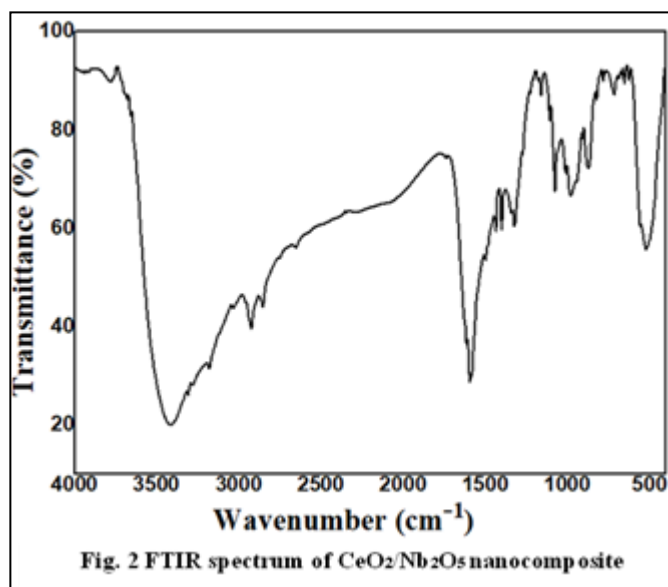


Fig. 2 FTIR spectrum of CeO<sub>2</sub>/Nb<sub>2</sub>O<sub>5</sub> nanocomposite

### 3.3 UV-Visible absorption analysis

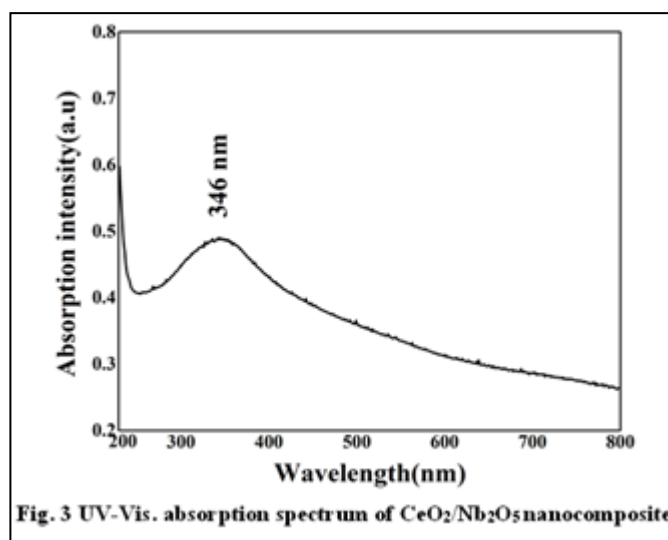


Fig. 3 UV-Vis. absorption spectrum of CeO<sub>2</sub>/Nb<sub>2</sub>O<sub>5</sub> nanocomposite

The optical properties of the synthesized CeO<sub>2</sub>/Nb<sub>2</sub>O<sub>5</sub> nanocomposite are determined from the absorption measurement in the UV-visible ranges from 200 to 800 nm. The UV-visible analysis is used to find the optical

transparency of the synthesized sample. The UV- vis. absorption spectrum of  $\text{CeO}_2/\text{Nb}_2\text{O}_5$  nanocomposite is depicted in the Fig. 3. The maximum absorption peak occurred at 346 nm. The band gap energy of  $\text{CeO}_2/\text{Nb}_2\text{O}_5$  nanocomposite is 3.59 eV.

### 3.4 HRSEM analysis

The HRSEM is employed to study surface morphology of the prepared  $\text{CeO}_2/\text{Nb}_2\text{O}_5$  nanocomposite. Fig. 4 shows the HRSEM image of  $\text{CeO}_2/\text{Nb}_2\text{O}_5$  nanocomposite with different magnifications (a)  $5\mu\text{m}$  and (b) 500 nm.

The HRSEM image shows the spherical like morphology and the estimated average particle size is 32 nm.

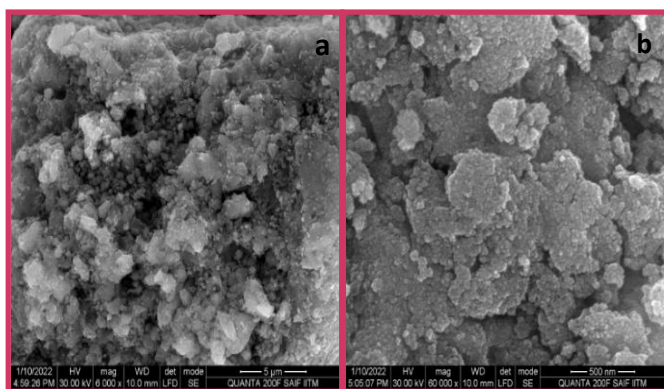


**Fig. 4 HRSEM image of  $\text{CeO}_2/\text{Nb}_2\text{O}_5$  nanocomposite with different magnification (a)  $5\mu\text{m}$  and (b) 500nm**

### 3. Conclusion

The  $\text{CeO}_2/\text{Nb}_2\text{O}_5$  nanocomposite is synthesized by co-precipitation method. The average crystallite size of the  $\text{CeO}_2/\text{Nb}_2\text{O}_5$  nanocomposite is 17.2 nm. The compositional analysis of the  $\text{CeO}_2/\text{Nb}_2\text{O}_5$  nanocomposite is studied by FTIR. The spherical morphology of the  $\text{CeO}_2/\text{Nb}_2\text{O}_5$  nanocomposite is observed by HRSEM analysis. From the UV-Vis. absorption analysis, the band gap energy of  $\text{CeO}_2/\text{Nb}_2\text{O}_5$  nanocomposite is estimated.

### Reference

- [1] P. M. Ajayan, L. S. Schadler, P. V. Braun, Nanocomposite science and technology. Wiley-VCH, (2003).
- [2] M. Alexandre, P. Dubois, Polymer-layered silicate nanocomposites: preparation, properties and uses of a new class of materials, *Materials Science and Engineering: R: Reports*, 28(1-2), 1-63, (2000).
- [3] S. S. Ray, M. Okamoto, Polymer/layered silicate nanocomposites: a review from preparation to processing. *Progress in Polymer Science*, 28(11), 1539-1641, (2003).
- [4] J. Jordan, K. I. Jacob, R. Tannenbaum, M. A. Sharaf, I. Jasiuk, Experimental trends in polymer nanocomposites—a review, *Materials Science and Engineering: A*, 393(1-2), 1-11, (2018).
- [5] M. Wang, Z. Li, X. Zhang, Y. Chen, Mechanics of Multifunctional Composites: A Review. *Composite Structures*, 284, 115148, (2022).
- [6] T. Liu, B. Zhao, J. Zhang, Y. Li, Recent Advances in Polymer Nanocomposites: From Fundamental Research to Practical Applications. *Progress in Materials Science*, 120, 100799, (2021).
- [7] G. Zhou, H. Chen, Y. Cui, Synergistic Nanocomposites for Advanced Lithium-Sulfur Batteries, *Chemical Society Reviews*, 52(5), 1623-1669, (2023).
- [8] Z. Wang, J. Smith, L. Johnson, K. Brown, Multifunctional Nanocomposites: Design, Fabrication, and Applications. *Advanced Materials*, 35(19), 2209659, (2023).
- [9] X. Zhang, L. Wang, C. Li, Z. Chen, Recent Advances in the Co-precipitation Synthesis of Nanocomposite Materials

for Energy Storage and Conversion Applications, Chemical Engineering Journal, 479, 147632, (2024).

[10] K.K. Kefeni, T.A. Msagati, B.B. Mamba, Ferrite na

noparticles: Synthesis, characterisation and applications in electronic device. Materials Science and Engineering: B, 215, 37–55, (2017).